Distribution Agreement

In presenting this thesis as a partial fulfillment of the requirements for a degree from Emory University, I hereby grant to Emory University and its agents the non-exclusive license to archive, make accessible, and display my thesis in whole or in part in all forms of media, now or hereafter known, including display on the world wide web. I understand that I may select some access restrictions as part of the online submission of this thesis. I retain all ownership rights to the copyright of the thesis. I also retain the right to use in future works (such as articles or books) all or part of this thesis.

Signature:

_____	_____
Zachary Hudson	April 22, 2010

Synthesis, Characterization, and Biological Data for Potential Anticancer Gold(III) Complexes.

by

Zachary Hudson

Adviser: Dr. Cora MacBeth

Department of Chemistry

_____
Cora MacBeth
Adviser

_____
Jack Eichler
Committee Member

_____
Pat Marsteller
Committee Member

_____
April 22, 2010

Synthesis, Characterization, and Biological Data for Potential Anticancer Gold(III) Complexes.

By

Zachary D. Hudson

Adviser: Dr. Cora Macbeth

An abstract of
A thesis submitted to the Faculty of Emory College of Arts and Sciences
of Emory University in partial fulfillment
of the requirements of the degree of
Bachelor of Arts with Honors

Department of Chemistry

2010

Abstract

Synthesis, Characterization, and Biological Data for Potential Anticancer Gold(III) Complexes.

By Zachary D. Hudson

In an effort to discover potential alternatives to the anti-cancer drug cisplatin, the synthesis of gold(III) polypyridyl coordination complexes was pursued. Specifically, this report describes the synthesis and characterization of a series of 2,9-dialkyl-1,10-phenanthroline gold(III) coordination complexes (R = *n*-butyl, *sec*-butyl, and *tert*-butyl), along with preliminary biological data. Due to the steric hindrance imparted by the alkyl subsitutents, these ligands do not react with $HAuCl_4$ to form square-planar gold(III) dichloride complex ions, as is the case with 1,10-phenanthroline, but instead form salts comprised of $[AuCl_4]$- anions and protonated 2,9-dialkylphenanthroline cations (compounds **1** and **2**). In an effort to facilitate direct binding between the substituted phenanthroline and the gold(III) metal center, reactions were carried out between the ligand and $NaAuCl_4$ in the presence of a Ag(I) salt. The precipitation of one equivalent of AgCl afforded the formation of neutral, distorted square pyramidal gold(III) trichloride complexes (compounds **3** and **4**). Substitutions which are 1° or 2° at the alpha carbon of the alkyl subsituent allow direct metal-ligand coordination, whereas a 3° substituent inhibits chelation and results only in the formation of a salt comprised of a protonated phenanthroline cation and an $[AuCl_2]$- anion (compound **5**). Compounds **1**-**4** have been characterized by ^{1}H NMR, UV-Vis, and IR spectroscopy, and X-ray crystallography. Assays probing cytotoxicity within existing tumor cell lines are reported herein, along with *in vitro* inhibition studies of the mitochondrial enzyme thioredoxin reductase.

Synthesis, Characterization, and Biological Data for Potential Anticancer Gold(III) Complexes.

By

Zachary Hudson

Adviser: Dr. Cora MacBeth

A thesis submitted to the Faculty of Emory College of Arts and Sciences
of Emory University in partial fulfillment
of the requirements of the degree of
Bachelor of Arts with Honors

Department of Chemistry

2010

Acknowledgents

I would like to thank the Oxford College Department of Chemistry, the Emory Department of Chemistry, the Summer Undergraduate Research Program at Emory, and Scholarly Inquiry and Research at Emory programs, and the Howard Hughes Medical Institute under grant 52005873 for providing funding for this project. I would also like to thank Dr. Scott Bunge of Kent State University and Dr. Kenneth Hardcastle of Emory University for solving the crystal structures, Melody Rhine for synthetic assistance, and Chinar Sangvhi for synthetic assistance and for providing the crystal structure to the 6,6'-dimethyl-2,2'-bipyridine gold(III) trichloride coordination complex. I would also like to thank Dr. Georgia Chen and her lab at the Winship Cancer Institute for the cytoxicity cell assays; and Dr. Elias Arnér and Dr. Stephanie Prast for the thioredoxin reductase activity assays. I also thank Dr Shaoxiong Wu and Dr Bing Wang at the Emory NMR center for their support and assistance.

I would especially like to thank my research mentors Dr. Jack Eichler and Dr. Cora MacBeth. Your guidance and support throughout have been invaluable to the success of this work. In addition, thank you for your mentorship, both personal and professional.

Table of Contents

Tables and Figures

1. Introduction

The platinum(II)-based *cis*-diamminedichloroplatinum (cisplatin) is widely regarded as one of the most successful metal-based cancer therapeutics, efficacious against a variety of cancers such as ovarian, testicular, and head and neck tumor **(**Figure 1**)**.[1,2] While it was one of the first metallotherapeutics to gain widespread use, it is not without its drawbacks. Cisplatin is highly damaging to rapidly dividing cells in the human body, and also exhibits nephrotoxicity and neurotoxicity.[3-5] In addition, tumors develop resistance, both *in vivo* and in *in vitro* tumor cell lines.[6] Due to these issues, it has become necessary to find new potential alternatives to cisplatin as a chemotherapy agent.

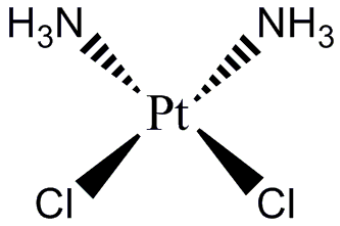

Figure 1. Structure of cisplatin.

Cisplatin has been shown to work as an anticancer agent via direct binding to DNA and interruption of its normal structure, thus interfering with normal transcription and copying.[7] The pathway of resistance is not currently fully explained, but is thought to work via means of increased concentration of the reductant glutathione in the cell, or via upregulation of oncogenes or DNA repair mechanisms.[7] Such resistance, once acquired, is very difficult to overcome, and so a natural plateau has been reached within platinum-based metallotherapies.

Due to the success of the metal-based cisplatin, and also due to its drawbacks, there has been an ongoing search for new metal-based chemotherapies. Ruthenium(II) complexes have been explored for their anticancer potential, particularly following a similar DNA binding mechanism to cisplatin.[8-12] Hartinger et al. have produced a ruthenium complex with two nitrogen donor ligands that has shown great preclinical potential as an antitumor agent and is currently in clinical trials (Figure 2).[13] Palladium(II) compounds have also been explored, showing potential due to their decreased impact on normal cells and decreased development of therapeutic resistance as compared to cisplatin.[14] Rhodium, copper, and lanthanum are also being explored, particularly with bis(N,N') donor ligands analogous to cisplatin.[15]

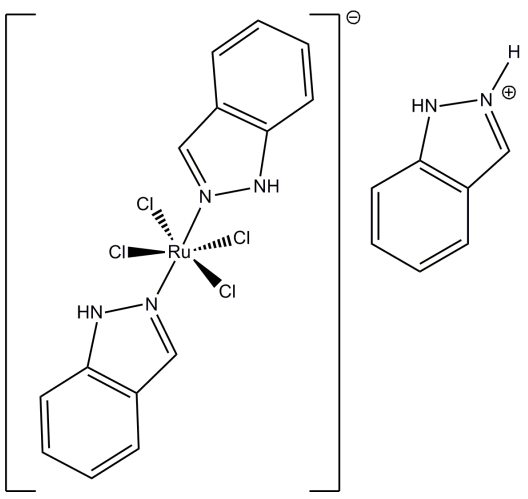

Figure 2. Ruthenium based antitumor agent possessing two nitrogen donor ligands currently undergoing clinical trials.[13]

Gold therapies have been historically used to treat rheumatoid arthritis which led to the discovery that such treatments also lowered the risk of several types of cancer, and subsequently to increased interest in their application as anticancer therapies.[16] Gold(III) compounds, in particular, are being explored because they are isoelectronic to the Pt(II)

ion found in cisplatin.[17] Thus it was originally thought that structural analogues of cisplatin would demonstrate a similar reaction mechanism, however, it has since been demonstrated that gold(III) coordination complexes tend to show a much lower binding affinity to DNA as compared to cisplatin.[18,19] Despite this, gold compounds appear to be a particularly strong avenue to pursue, since gold complexes tend to have strong cytotoxic potential in the micromolar or even nanomolar ranges.[20] Indeed, gold complexes appear to be more cytotoxic than other analogous, isoelectronic metal complexes.[21]

The exact mechanism of gold(III) coordination compound interaction with the cellular environment is unknown, but several theories have been proposed. As it appears that such complexes have a strong affinity for certain proteasomes, direct proteasome inhibition has been proposed.[22] Such complexes also appear to have a particularly high affinity for the unique selenocysteine residue in the mitochondrial enzyme thioredoxin reductase (TrxR), and thus inhibition of mitochondrial function through an interaction with TrxR has been proposed.[22,23] Other works have also suggested that gold(III) compounds introduce apoptosis via an unspecified effect on mitochondrial function.[24] In addition, it appears that gold(III) porphyrins might induce cell death through interaction with nitrogen-activated protein kinase proteins.[25]

In this study, we have chosen to explore polypyridyl gold(III) anologues of cisplatin, using derivatives of 1,10-phenanthroline (phen) as a bis(N,N') donor ligand (Figure 3). Phen derivatives using other metals, such as Rh, Cu, and Pd are being currently explored for their potential.[15,26-28] The dichloride gold(III) phen coordinate complex ion (Figure 3) has been previously found to be stable at physiological pH and

temperature for at least several hours, with possible exchange of the chloride ligands for hydroxo ligands, while also possessing strong cytotoxic potential anticancer properties.[29] A recent study has demonstrated the very high cytotoxic potential of gold(III) phen and shown that its mechanism of action is not correlated with that of DNA binding. It might be due to inhibition of cyclin-dependent kinases within the cellular environment, interrupting the cellular cycle and inducing apoptosis, but this remains inconclusive. While it demonstrated high cytotoxic potential within this study, it did not have high target specificity against specific tumor cell lines and instead showed similar cytotoxic potential across a variety of tumor cell lines.[30] Thus, it is thought that modification to the structure of gold(III) phen might alter this specificity, either enhancing or depressing it and providing a means of probing its mechanism of action and enhancing its biological potential as an anticancer agent against a more narrow line of target cells.

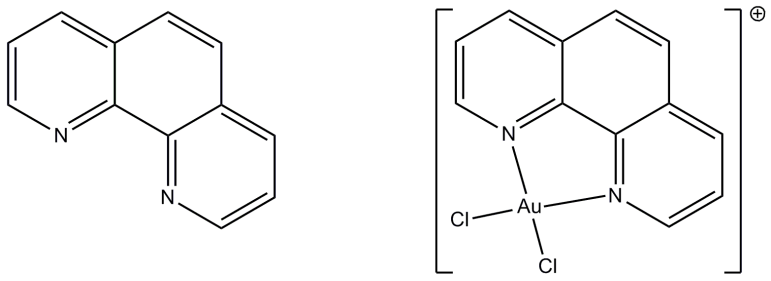

Figure 3. Structure of the unsubstituted 1,10-phenanthroline ligand (left) and the square planar 1,10-phenanthroline gold(III) dichloride coordinate ion (right).

To our knowledge, only one example of a structurally characterized 2,9-alkyl-1,10-phenanthroline derivative has been published.[31] This methyl derivative favored a neutral, distorted square-pyramidal geometry possessing three chloride ligands and bis(N,N') donor ligand vs. the unsubstituted phen complex which has an ionic square-planar geometry possessing two chloride ligands, and the bis(N,N') donor ligand with a

chloride counter-ion.[31] No analogues using bulkier substituents were present in the literature previous to our studies, and thus phenanthroline ligands possessing bulkier alkyl substitutions were chosen. The ligands themselves could be synthesized with relative ease using a previously published procedure.[32] It was thought that exploring such a substitution would be useful for several reasons. The positioning of the alkyl groups is thought to have the potential to sterically protect the metal center against the reduction potential of glutathione and ascorbic acid within the cellular environment, as is thought to be one of the possible mechanisms of cisplatin resistance. In addition, such substituents provide means to alter the structure and might improve the potential *in vivo* effects of the complexes. This can also allow for the probing of DNA interactions, because if the metal center interacts directly with DNA in the unsubstituted complex then the alky groups should block this DNA binding. If DNA interaction is not the main mechanism of apoptosis and the metallotherapeutic potential is instead derived from a mechanism such as enzyme inhibition, then this could also control for the potentially unwanted side effect of DNA interaction *in vivo*.

Given that 2,9-dimethyl-1,10-phen gold(III) trichloride is the only other known instance of a 2,9-substituted phen gold(III) complex, we sought to create analogous complexes using *n*, *sec*, and *tert*-butyl alky substituents. Initial attempts yielded a protonated phenanthroline cation with an gold(III) tetrachloride anion ($PhenH^{+}AuCl_4^{-}$) This thesis will discuss the synthesis and characterization efforts of the initial salts, where the alkyl substitutions are n-butyl and sec-butyl (compounds **1** and **2**), and a new procedure for the synthesis of novel neutral substituted phenanthroline gold(III) chloride coordination species with analogous substitutions (compounds **3** and **4**) (Figure 3).

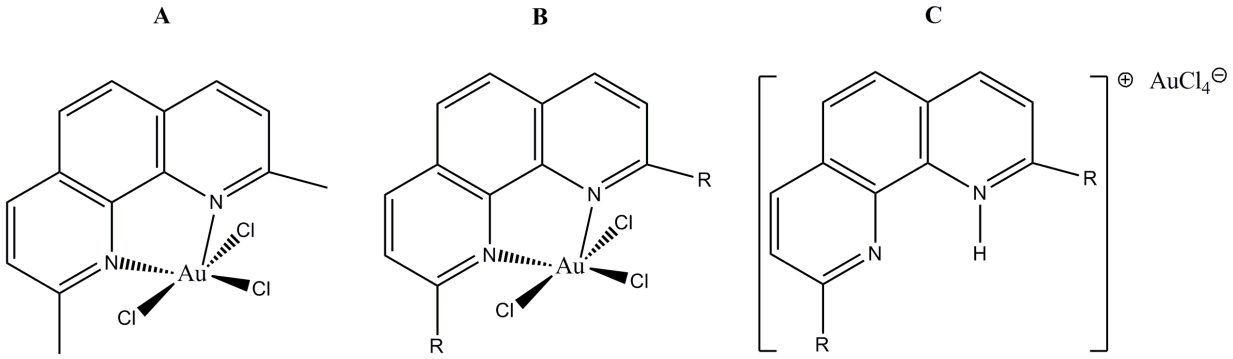

Figure 4. A.) 2,9-dimethyl-1,10-phenanthroline $AuCl_3$ complex.[31] B.) New 2,9-dialkyl-1,10-phenanthroline complexes (R = *n*-butyl (**3**) and *sec*-butyl (**4**). C. Protonated phenanthroline ($PhenH^+$) salts (R = *n*-butyl (**1**) and *sec*-butyl (**2**).

2. Experimental

2.1 General Procedures

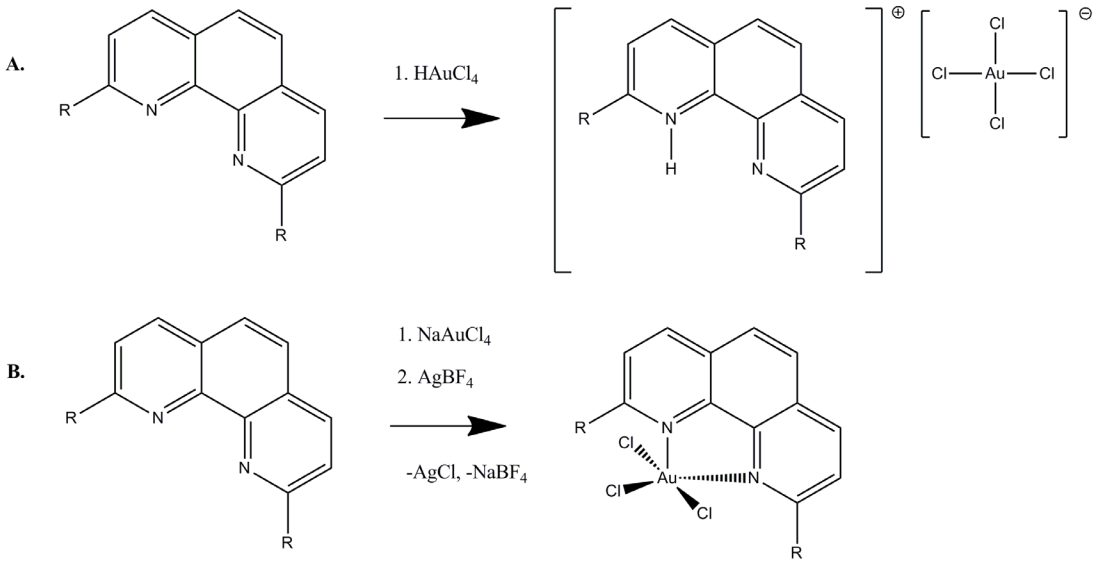

Scheme 1. Reaction schema for the syntheses of A) [^{R}phenH][$AuCl_4$] salts (**1**, **2**) and B) the neutral, distorted square pyramidal [Au(^{R}phen)Cl_3] complexes (**3**, **4**) (**1** and **3**, R = *n*-butyl; **2** and **4**, R = *sec*-butyl).

The 2,9-dialkylphen ligands (alkyl = *n*-butyl, *sec*-butyl, *tert*-butyl) were synthesized as described in the literature.[32] $HAuCl_4{\cdot}3H_20$, $NaAuCl_4{\cdot}2H_2O$, silver

tetrafluoroborate, silver trifluoroacetate (Alfa Aesar), and all solvents were used without further purification. The gold starting materials were weighed and solvated under a nitrogen atmosphere (either in an inert atmosphere glovebox or in a nitrogen-purged glovebag) and subsequently refluxed in normal atmospheric conditions with the appropriate phen ligand. Aside from eliminating exposure to direct sunlight, no special handling measures were taken with the final gold(III) complexes. ^{1}H-NMR spectra were recorded on a Varian Mercury 300 MHz spectrophotometer at ambient temperature; chemical shifts were referenced to residual solvent peaks. Infrared spectra were recorded as KBr pellets on a Varian Scimitar 800 Series FT-IR Spectrophotometer, UV/VIS spectra were recorded on a Cary 50 UV/VIS spectrophotometer using 1.0 cm quartz cuvettes, and elemental analyses were completed by Atlantic Microlab Inc., Norcross, GA.

2.2 X-ray Crystallography (compounds 1 and 2)[33]

X-ray crystallography was performed by mounting each crystal onto a thin glass fiber from a pool of Fluorolube™ and immediately placing it under a liquid nitrogen cooled N_2 stream, on a Bruker AXS diffractometer. The radiation used was graphite monochromatized Mo Kα radiation (α = 0.7107 Å). The lattice parameters were optimized from a least-squares calculation on carefully centered reflections. Lattice determination, data collection, structure refinement, scaling, and data reduction were carried out using APEX2 version 1.0-27 software package.

Each structure was solved using direct methods. This procedure yielded the Au atoms, along with a number of the Cl, N, and C atoms. Subsequent Fourier synthesis

yielded the remaining atom positions. The hydrogen atoms were fixed in positions of ideal geometry and refined within the XSHELL software. These idealized hydrogen atoms had their isotropic temperature factors fixed at 1.2 or 1.5 times the equivalent isotropic U of the C atoms to which they were bonded. The final refinement of each compound included anisotropic thermal parameters on all non-hydrogen atoms.

2.3 X-ray Crystallography (compounds 3-5)

For X-ray crystallography, suitable crystals of **3-5** were coated with Paratone N oil, suspended in a small fiber loop and placed in a cooled nitrogen gas stream at 173 K on a Bruker D8 APEX II CCD sealed tube diffractometer with graphite monochromated CuK_α (1.54178 Å) radiation. Data were measured using a series of combinations of phi and omega scans with 10 s frame exposures and 0.5^o frame widths. Data collection, indexing and initial cell refinements were all carried out using APEX II software.[34] Frame integration and final cell refinements were done using SAINT software.[34] The structure was solved using direct methods and difference Fourier techniques (SHELXTL, V6.12).[35] Hydrogen atoms were placed in their expected chemical positions using the HFIX command and were included in the final cycles of least squares with isotropic U_{ij}'s related to the atom's ridden upon. All non-hydrogen atoms were refined anisotropically. Scattering factors and anomalous dispersion corrections are taken from the *International Tables for X-ray Crystallography*. Structure solution, refinement, graphics and generation of publication materials were performed by using SHELXTL, V6.12 software.

2.4 Synthesis of Compound 1

2,9-di-*n*-butyl-1,10-phenanthroline (0.340 g, 1.2 mmol) was dissolved in 15 mL of MeOH and added dropwise to $HAuCl_4 \cdot 3H_2O$ (0.447 g, 1.2 mmol) in 20 mL of MeOH,

upon which a deep purple solution was produced. After refluxing for 1 hour at 80 °C, the solution turned dark yellow. Evaporation *in vacuo* produced a red/orange pasty solid, which was washed with 20 mL of ether (the ether wash was discarded). A yellow solid (**1**) was isolated and then dried under vacuum at 35 °C (0.361g, 49%). Yellow needles suitable for X-ray diffraction studies were obtained by slow-evaporation from dichloromethane. Elemental analysis found: C, 38.27%; H, 3.98%; calculated: C, 37.98%; H 3.99%. $\lambda_{max}(MeCl_2)$/nm 232.0 (26 070), 289.0 (20 150) and 318.0sh (6 800). IR: ν_{max}/cm^{-1} 3178 (NH), 3073 (CH), 2958, 2930, 2872 (CH), 1624, 1605 (conj. CC). ^{1}H NMR (300 MHz, dmso) δ 8.85 – 8.79 (m, 2H, H-7,12), 8.17 (s, 2H, H-9,10), 8.06 – 7.99 (m, 2H, H-6,13), 3.26 (s, 4H, H-4,15), 1.81 (s, 4H, H-3,16), 1.42 (d, 4H, H-2,17), 0.94 (t, 6H, H-1,18) (See Figure 5 for NMR numbering scheme).

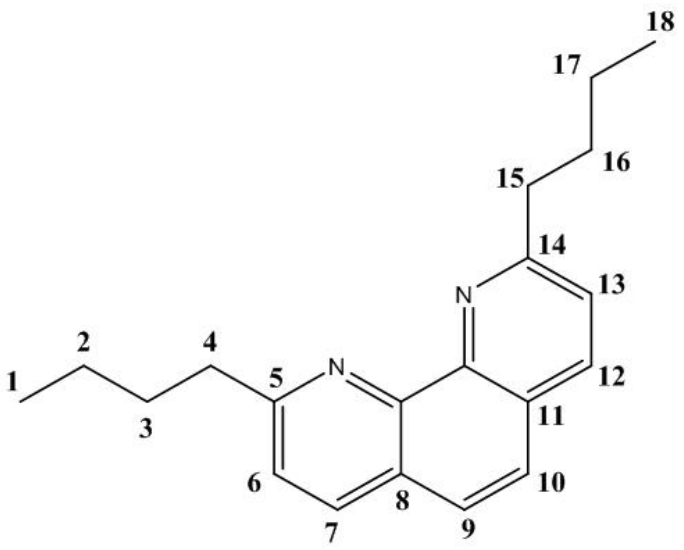

Figure 5. NMR numbering scheme for **1** and **3**. Hydrogens are labeled according to the carbon they are directly bonded to.

2.5 Synthesis of Compound 2

2,9-di-*sec*-butyl-1,10-phenanthroline (0.523 g, 1.8 mmol) and $HAuCl_4 \cdot 3H_2O$ (0.705 g, 1.8 mmol) were combined in a procedure analogous to the synthesis of **1**, yielding 0.900 g of a reddish/orange solid, **2** (79.6%). Yellow needles suitable for X-ray diffraction studies were obtained by slow-evaporation from dichloromethane. Elemental analysis found: C, 37.99%; H, 3.99%; calculated: C, 37.98%; H, 3.99%. λmax($MeCl_2$)/nm 231.0 (33 670), 287.9 (31 440) and 319.1 (11 770). IR: ν_{max}/cm^{-1} 3183 (NH), 3079 (CH), 2963, 2928, 2871 (CH), 1619, 1602 (conj. CC). ^{1}H NMR (300 MHz, cdcl3) δ 8.88 (d, 2H, H-7,12), 8.24 (s, 2H, H-9,10), 8.06 (d, 2H, H-6,13), 3.75 (m, 14.2, 2H, H-3,15), 2.09 (m, 13.7, 2H, H-2), 1.86 – 1.68 (m, 2H, H-17), 1.48 (d, 6H, H-4,16), 0.93 (t, J = 7.4, 6H, H-1,18) (See Figure 6 for NMR numbering scheme).

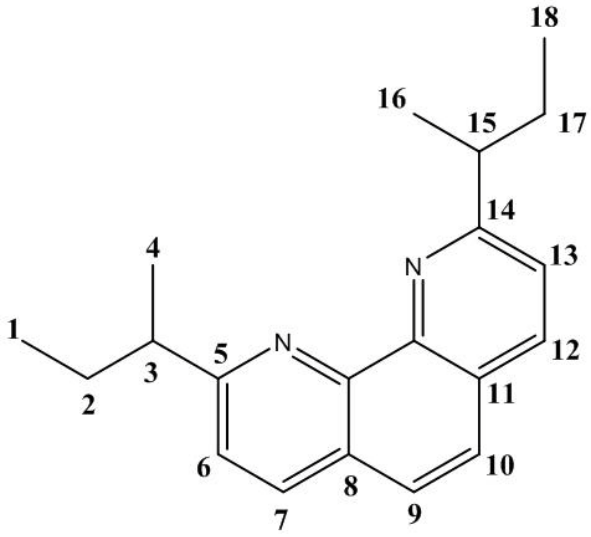

Figure 6. NMR numbering scheme for **2** and **4**. Hydrogens are labeled according to the carbon they are directly bonded to.

2.6 Synthesis Compound 3

2,9-di-*n*-butyl-1,10-phenanthroline (0.265 g, 0.900 mmol) and $NaAuCl_4 \cdot 2H_2O$ (0.365 g, 0.900 mmol) were added to 50 ml of acetonitrile, upon which a brown solution was produced. This reaction mixture was refluxed for 1 hour, and $AgBF_4$ (0.176 g, 0.9 mmol) was dissolved in acetonitrile and delivered to the reaction solution. The final reaction mixture was refluxed overnight, and the precipitate (AgCl) was filtered off with a celite pad. A liquid-liquid extraction ($MeCl_2$:H_2O, 20mL of each) was performed, and the aqueous layer was discarded. A red/orange viscous paste remained after removal of the organic phase *in vacuo*. This crude product was washed with a small amount of methanol, leaving behind a red solid. The methanol wash was discarded and the solid was dried under vacuum to give **3** (0.313g, 58%). Orange needles suitable for X-ray diffraction studies were obtained by slow-evaporation from ethanol. MP: 134 °C (EtOH). Elemental analysis found: C, 40.33%, H 3.99%; calculated: C, 40.30%, H, 4.06%. $\lambda_{max}(MeCl_2)$/nm 233 (27 320), 279 (24 560) and 300sh (7 960) IR: ν_{max}/cm^{-1} 3052 (CH), 2957, 2929, and 2860 (CH), 1619 and 1594 (conj. CC). ^{1}H NMR (300 MHz, cdcl3) δ 8.53 (d, 2H, H-7,12), 7.98 (d, 2H, H-9,10), 7.80 (d, 2H, H-6,13), 3.79 (m, 4H, H-4,15), 2.01 – 1.87 (m, 4H, H-3,16), 1.57 – 1.42 (m, 4H, H-2,17), 1.03 (td, 7.3, 6H, H-1,18) (See Figure 5 for NMR numbering scheme).

2.7 Synthesis of Compound 4

2,9-*sec*-butyl-1,10-phenanthroline (0.199 g, 0.681 mmol) and $NaAuCl_4 \cdot 2H_2O$ (0.271g, 0.681 mmol) were added to 50 mL of acetonitrile, upon which a deep purple solution was produced. The addition of silver trifluoroacetate (0.150g, 0.681 mmol) produced a cloudy green solution, which developed into a pale yellow solution after

refluxing at 65 °C for 6 hours. A filtration and liquid-liquid extraction were performed as described for **3**, yielding a red-orange solid, **4** (0.371g, 86%). Orange needles suitable for X-ray diffraction studies were obtained by slow-evaporation from ethanol. MP: 137 °C (EtOH). Elemental analysis found: C, 40.42%, H 4.12%; calculated: C, 40.30%, H, 4.06%. $\lambda_{max}(MeCl_2)$/nm 232 (27 160), 278 (25 910) and 301sh (812). IR: ν_{max}/cm^{-1} 3067 (CH), 2964, 2930, 2871 (CH), 1623, 1595 (conj. CC). ^{1}H NMR (300 MHz, cdcl3) δ 8.43 (d, 2H, H-7,13), 7.93 (s, 2H, H-6,13), 7.83 (d, 2H, H-9,10), 4.50 (m, 2H, H-3,15), 1.98 – 1.80 (m, 14.4, 2H, H-2), 1.72 – 1.55 (m, 15.3, 2H, H-17), 1.42 (d, 6H, H-4,16), 0.99 (t, 6H, H-1,18) (See Figure 6 for NMR numbering scheme)

2.8 Synthesis of Compound 5

2,9-di-*tert*-butyl-1,10-phenanthroline (0.125 g, 0.43 mmol) was combined with $NaAuCl_4 \cdot 2H_2O$ (0.170 g (0.43 mmol) in acetonitrile with a procedure analogous to the synthesis of **4**, upon which a brown solution was produced. After refluxing, $AgBF_4$ (0.083 g (0.43 mmol) was added, yielding a grey precipitate. The solution was refluxed overnight, dried *in vacuo*, yielding a brown/yellow solid. Yellow needles suitable for X-ray diffraction were obtained by slow evaporation out of ethanol (0.100g, 42%).

2.9 Cytotoxicity Assays

Dimethyl sulphoxide (DMSO) and all cell culture reagents and media were purchased from Sigma-Aldrich. To test the effects of compounds **1-4** on cell growth of head, neck, and lung cancer cell lines, sulforhodamine B (SRB) cytotoxicity assays were adapted from Skehan et al. and compared to cisplatin and the starting ligand and $NaAuCl_4$ starting materials.[36] Twenty-five cells maintained in medium with 5% FBS were seeded in 96-well plates at a density of 4,000 cells/well overnight prior to drug

treatment. Afterwards, drugs were added in a range of concentrations as single agents in various concentrations (0–30 micromolar), followed by incubation at 37°C and 5% CO2 for 72 hours. Cells were fixed for 1 hr with 10% cold trichloroacetic acid. Plates were washed 5 times in water, air-dried and then stained with 0.4% SRB for 10 min. After washing 4 times in 1% acetic acid and air-drying, bound SRB was dissolved in 10 mM unbuffered Tris base (pH 10.5). Plates were read in a microplate reader by measuring absorbance at 492 nm. Cell growth inhibition was measured by determining cell density with sulforhodamine B assay at 72 hours after addition of the drugs. Percentage of inhibition was determined by comparison of cell density in the drug-treated cells with that in the untreated cell controls in the same incubation period. The percent survival was then calculated based upon the absorbance values relative to untreated samples. The experiment was repeated 3 times.[37]

2.10 Thioredoxin Reductase Assay[38]

Compounds **1, 2**, and **4** were prepared in 4 mL (10 mg/mL DMSO). NaAuCl4, and KAuCl4 were used as controls. For inhibition of TrxR, 50 nM recombinant rat TrxR1 (8.3 U/mg) was reduced by the addition of 250 μM NADPH to the assay buffer (50 mM Tris pH 7.5, 2 mM EDTA) and subsequently incubated 15 min at room temperature with increasing concentrations of the compounds. Two aliquots of 195 μL were subjected to a microtiter plate and 250 μM NADPH and 2.5 mM DTNB was added. Immediately, the DTNB reduction to TNB^- was followed at 30° C for 5 min at 412 nm using the VersaMax (Molecular devices). A linear slope was calculated for the same 30 s interval of all samples within one run and the percentage of activity compared to enzyme incubated with assay buffer only was calculated for all treated samples.

3. Results and Discussion

3.1 Synthesis and Spectroscopic Characterization

A 1:1 molar ratio of 2,9-dialkylphen (alkyl = *n*-butyl, *sec*-butyl) and $HAuCl_4$ was refluxed in methanol, yielding a $phenH^+/AuCl_4^-$ salt (Scheme 1A); this is in contrast to the successful metal-ligand chelation reported for unsubstituted phenanthroline.[29] The difference in reactivity may be explained both by issues of steric hindrance introduced by the substitution and by the increase in nitrogen basicity by the addition of alkyl groups to the aromatic ligand backbone. Refluxing molar equivalents of *n*-butyl and *sec*-butylphen with $NaAuCl_4$, along with silver(I) salts in acetonitrile, yielded neutral phen gold(III) trichloride coordination complexes (Scheme 2A), while the use of the analogous synthetic procedure with 2,9-di-*tert*-butyl substituted ligand yielded a $phenH^+/AuCl_2^-$ salt (**5**).

The synthesis of gold(III) salts possessing protonated nitrogen donor ligands, such as compounds **1** and **2**, is not unprecedented. Cao, *et al*. recently reported the reaction of $HAuCl_4$ with bis(2-pyridylmethyl)-N-benzylamine (BBPMA), which resulted in a salt complex of $AuCl_4^-$ and the protonated BBPMA ligand.[39] However, these authors were also able to obtain direct coordination between the ligand and gold(III) metal center by using $NaAuCl_4$ instead of $HAuCl_4$.[39] The synthesis of 2,9-di-methylphen gold(III)trichloride (Figure 4A), a structural analogue of compounds **3** and **4**, was originally carried out using $KAuCl_4$, however these authors did not require the use of a silver(I) salt to facilitate direct coordination of the substituted phen ligand (in our hands, gold(III) complexes were only isolable using silver(I) salts) [31]

In comparison to the free phen ligands, a general downfield shift occurs for the aromatic and alkyl hydrogens in both the $AuCl_4^-$ salts and the neutral $AuCl_3$ complexes

[di-*sec*-butylphen ligand: δ 8.12, 7.68, 7.48 (aromatic), 3.31(-CH); compound **2**: δ 8.88, 8.24, 8.06 (aromatic), 3.75 (-CH); compound **4**: δ 8.43, 7.93, 7.83(aromatic), 4.50(-CH)]. Given the expected downfield shift of the ligand protons upon coordination to a cationic metal center [CuCl(di-*sec*-butylphen)$_2$: δ 8.73, 8.15, 7.77 (aromatic), 3.01(-CH)] [32], the ^{1}H NMR data for **1** and **2** was originally interpreted as evidence that the phen was directly coordinated to the gold(III) cation (Figure 7). However, after characterizing compounds **1** and **2** using IR [**1**: ν = 3178 cm^{-1} (N-H); **2**: ν = 3183 cm^{-1}(N-H)], as well as elemental analysis (see experimental) and X-ray crystallography (Figures 9-10), it was found that the use of $HAuCl_4$ led to the formation of $phenH^+/AuCl_4^-$ salts.

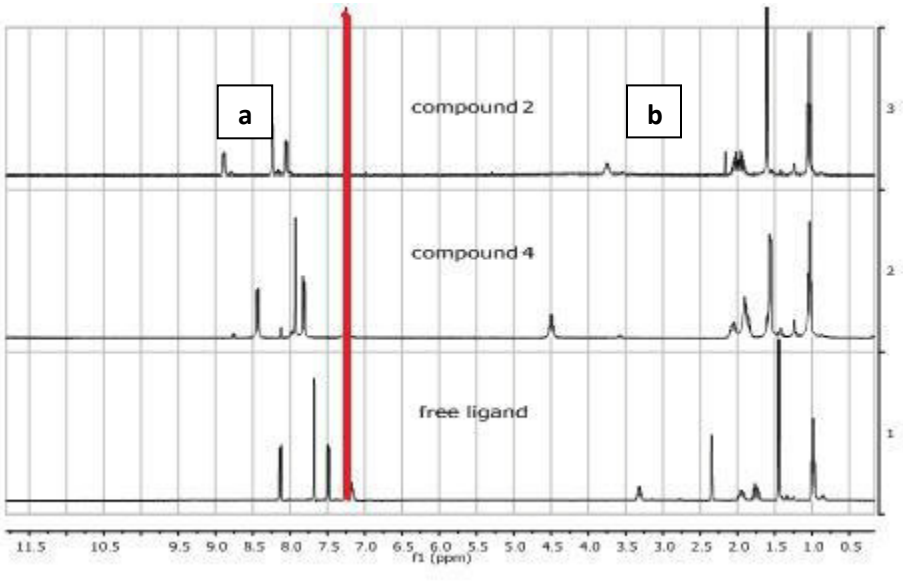

Figure 7. ^{1}H NMR spectra of compounds 2, 4, and the free $^{sec\text{-}Bu}$Phen ligand ($CDCl_3$, 20ºC; residual chloroform resonances are overlayed in red; (a)denotes the most downfield aromatic $^{sec\text{-}Bu}$Phen hydrogen and (b) denotes the –CH hydrogen from the *sec*-butyl pendant).

Given these results, we caution against the use of ^{1}H NMR as a singular diagnostic of phen coordination to gold(III), especially if $HAuCl_4$ is used as the gold source. Previous reports have described the reaction of substituted phen ligands with $HAuCl_4$ and claim that the substituted phen was directly bound to the Au(III) center.[11,40]

However, this was deduced only by ^{1}H-NMR studies; without additional structural characterization, it may not be prudent to make such a conclusion.

The characterization of compounds **1**-**4** by UV/VIS further demonstrated the difficulty in using spectroscopic data to determine if coordination of the phen ligand occurred. Comparison of the UV-visible absorption spectra of compounds **1** and **3** and compounds **2** and **4** reveal the close similarity of the absroption properties of the [^{R}phenH][$AuCl_4$] salts and the neutral [Au(^{R}phen)Cl_3] complexes (Figure 8). The [^{R}phenH][$AuCl_4$] salts (**1** and **2**) possess a series of strong absorption maxima at approximately 225-230, 270-275, and 280-285 nm, assigned as intraligand phen $\pi \rightarrow \pi^*$ transitions; and 320 nm, assigned as a Cl-Au LMCT band (it is noted that the $NaAuCl_4$ starting material exhibits a similar Cl-Au LMCT at approximately 320 nm).[16,20] The [Au(^{R}phen)Cl_3] complexes (**3** and **4**) displayed absorption maxima that were not clearly distinguishable from those observed in **1** and **2** [the intraligand transitions were observed at 225, 270-275, and 280-285 nm; and the LMCT bands were observed at approximately 320 nm]. The difference in the electronic properties of these two types of compounds is evidenced by the distinct difference in color between the two classes of compounds (**1** and **2** are bright yellow; **3** and **4** are orange), presumed to be differences in the d-d transitions, though this is not clearly discernable in the UV-visible absorption spectra.

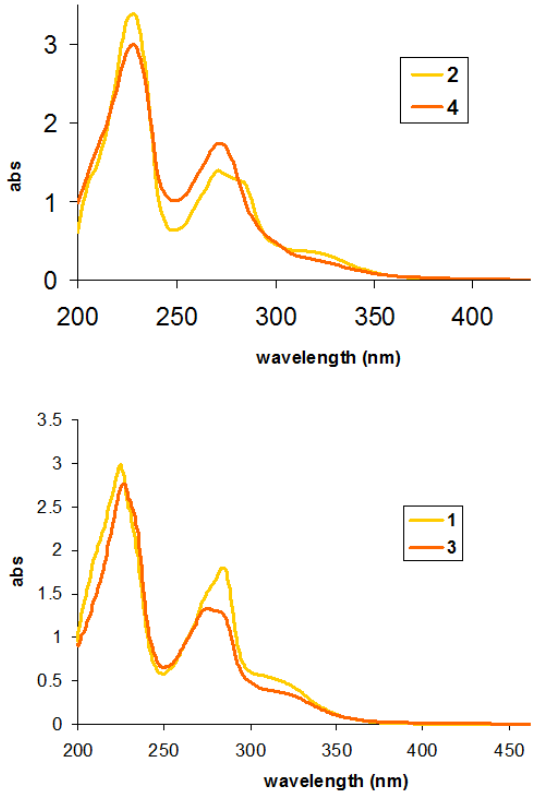

Figure 8. UV/Vis spectroscopic data of compounds **2** vs **4** and **1** vs **3**. The compounds were dissolved in a 3:1 2-propanol/acetonitrile mixture at 50 µM.

Compounds **3** and **4** displayed similar spectra, however there were noticeable shifts in the phen intraligand π → π* transitions [λ_{max} = 279 (**3**), 278 (**4**)] and the LMCT bands [λ_{max} = 300 (**3**), 301 (**4**)]. There was also a slight decrease in energy of the d-d transition, evidenced by the distinct difference in color between the two classes of compounds (**1** and **2** are bright yellow; **3** and **4** are orange). The higher energy π → π* transition in **3** and **4** is likely caused by an increase in the energy gap between the ligand π and π* orbitals, which would be expected upon direct coordination of the ligand to the gold(III) metal center. The increase in the energy of the LMCT is presumed to arise in **3** and **4** because the vacant d_{x2-y2} orbital, the recipient of the charge

transfer, is likely raised in energy upon coordination of the phen ligand (the phen nitrogen donor is a stronger field ligand than chloride). The decrease in energy of the d-d transition for the phen $AuCl_3$ complexes is most likely caused by the interaction of the axial phen nitrogen donor with the gold(III) cation. The direct interaction of this nitrogen lone pair would be expected to significantly raise the energy of the filled d_{z2} orbital, thereby reducing the energy gap between the d_{z2} and the empty d_{x2-y2} orbital.

3.2 X-ray Crystal Structures

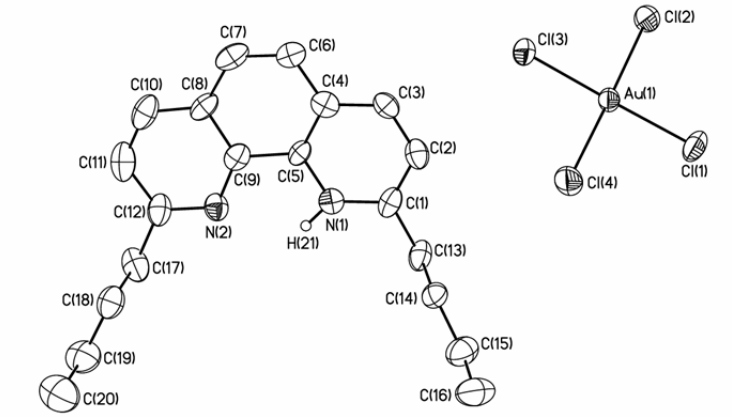

Figure 9. Molecular structure and numbering scheme of **1**. (35% probability) Hydrogen atoms have been omitted for clarity. Selected bond lengths (Å) and angles (°): Au-Cl···H-N 2.906, Au(1)–Cl(2) 2.271(3), Au(1)–Cl(3) 2.273(3), Au(1)–Cl(1) 2.275(3), Au(1)–Cl(4) 2.278(3), Cl(2)–Au(1)–Cl(3) 88.85(10), Cl(2)–Au(1)–Cl(1) 90.30(11), Cl(3)–Au(1)–Cl(1) 178.79(13), Cl(2)–Au(1) –Cl(4) 178.43(12).

Though $phenH^+$ salts have been structurally characterized with other metals, compounds **1** and **2** appear to be the first examples reported with the $AuCl_4^-$ anion (Figures 9-10). However, salts of $AuCl_4^-$ have been reported for other protonated nitrogen donor ligands, including protonated bipyridine,[22] protonated bis(2-pyridylmethyl)amine,[11] and protonated N-benzyl-C(2-pyridyl)nitrone.[41] Analogous to these structures, compounds **1** and **2** feature a square planar $AuCl_4^-$ anion (Figures 9-10).

However, **1** and **2** are, to our knowledge, the only examples of $AuCl_4^-$ salts possessing a hydrogen bond between one of the chloride ligands and the protonated nitrogen donor ligand; compound **1** and **2** possess Au-Cl···H-N interatomic distances of 2.906 Å and 3.000 Å, respectively. According to a review of M-Cl···H-N interactions from the crystallographic database, completed by Aullón *et al*., the hydrogen bonds in **1** and **2** are characterized as intermediate to long (M-Cl···H-N distances from 2.52-2.95 Å are classified as intermediate, and 2.95-3.15 Å are classified as long).[42]

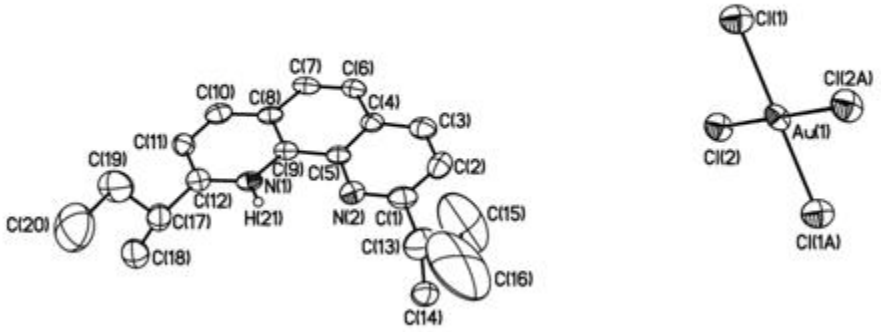

Figure 10. Molecular structure and numbering scheme of **2**. (35% probability) Hydrogen atoms have been omitted for clarity. Selected bond lengths (Å) and angles: Selected bond lengths (Å) and angles (°) for 2: Au-Cl...H–N 3.000, Au(1)–Cl(1) 2.278(2), Au(1) –Cl(2) 2.2807(18), Au(2)–Cl(3) 2.273(2), Au(2)– Cl(4) 2.277(2), Cl(1) –Au(1) –Cl(2) 90.34(7).

As described above, the use of $NaAuCl_4$ and silver(I) salts in the synthetic protocol afforded direct coordination of the di-*n*-butylphen (**3**) and di-*sec*-butylphen (**4**) ligands to gold(III). The coordination environment of **3** and **4** was determined by X-ray crystallography to be distorted square-pyramidal, where three chloride ligands and one of the phen nitrogen donors occupy the coordination sites on the base of the square pyramid, and the remaining phen nitrogen donor lies in the axial position (Figures 11-12). These compounds are structural analogues of the di-methyl-phen gold(III)trichloride (DMP-

gold) previously reported by Robinson, *et al*.[31] The formation of the distorted square planar geometry is likely caused by steric hindrance introduced by the alkyl substituents on the phen ligand.

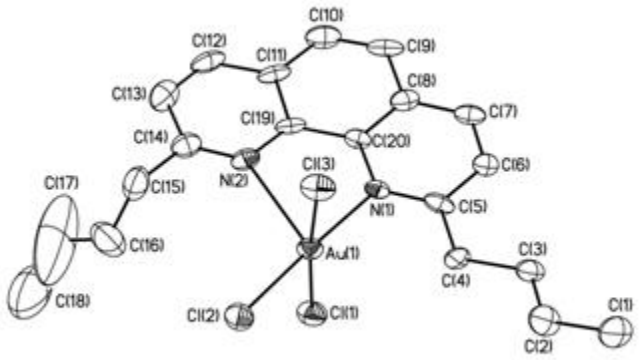

Figure 11. Molecular structure and numbering scheme of **3**. (35% probability) Hydrogen atoms have been omitted for clarity. Selected bond lengths (Å) and angles (°): Au(1)–N(1) 2.066(9), Au(1)–N(2) 2.597(9), Au(1)–Cl(2) 2.273(3), Au(1)–Cl(1) 2.291(3), Au(1)–Cl(3) 2.296(3), Au(1)–N(2) 2.597(9), N(1)–Au(1)–Cl(2)177.7(3), N(1)–Au(1)–Cl(1)89.6(3), Cl(2)–Au(1)–Cl(3)91.87(13), Cl(1)–Au(1)-Cl(3)174.31(12).

Structurally characterized gold(III) complexes possessing this distorted square pyramidal geometry are quite rare (only six gold(III) structures possessing two nitrogen donor ligands and three halide ligands can be found on the CCDC),[43-45] and compounds **3** and **4**, along with DMP-gold, represent the only examples bearing substituted phen ligands. The noteworthy feature of these complexes, as previously reported by Robinson [31], is the elongation of the Au-N_{axial} bond [average Au-N_{axial}: 2.594 Å (**3**); 2.583 Å (**4**); 2.584 Å (DMP-gold)] , and the "lean" of the square pyramid [angle of Au-N_{axial} axis to the plane of square pyramid base: 73.2º, 109.1º (**3**); 73.0º, 110.4º (**4**); 73.4º, 111.1º (DMP-gold)]. This is thought to be caused by the electron repulsion between the filled

d_z^2 orbital and loan pairs from the axial nitrogen donor, as well as the steric influence of the phen alkyl groups. The Au-Cl interatomic distances are in a range expected for square pyramidal geometry [range of Au-Cl distances: 2.262-2.300 Å (**3**); 2.256-2.312 Å (**4**); 2.267-2.2.285 Å (DMP-gold) [31]].

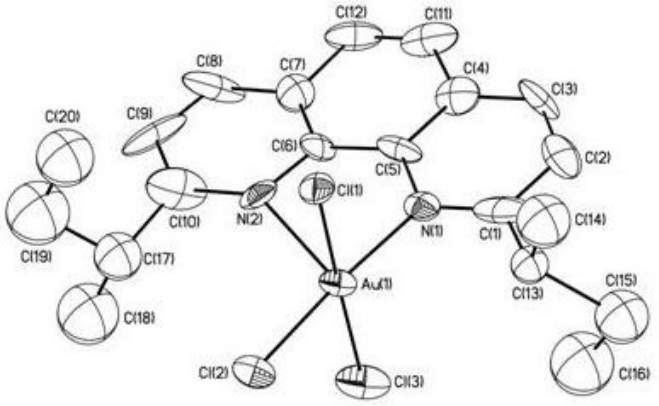

Figure 12. Molecular structure and numbering scheme of **4**. (35% probability) Hydrogen atoms have been omitted for clarity. Selected bond lengths (Å) and angles (°): Au(1)–N(1) 2.063(15), Au(1)–N(2) 2.598(18), Au(1)– Cl(1) 2.285(5), Au(1)–Cl(2) 2.265(5), Au(1)–Cl(3) 2.275(6), N(1)–Au(1)–Cl(1) 90.7(5), N(1)–Au(1)–Cl(2) 175.6(6), Cl(1)–Au(1)–Cl(2)89.9(2), N(1)–Au(1)–Cl(3)88.9(5), Cl(1)–Au(1)–Cl(3)176.3(3).

Attempts to synthesize the neutral square pyramidal gold(III) complex with 2,9-di-*tert*-butylphen were not successful in our laboratory. In fact, even when silver(I) salts were used to encourage coordination of the phen ligand, the only product that could be isolated was a reduced gold species comprised of a linear $AuCl_2^-$ anion and a protonated di-*tert*-butylphen ligand; given the bulk of the *tert*-butyl groups, this was not a surprising result. The effect of the steric bulk of this phen ligand can be seen by comparing the Au-Cl···H-N hydrogen bonding distance of **5** (3.459 Å) to that observed in **1** and **2** (2.906 Å and 3.000 Å). A similar complex was reported by Cao *et al* [39], in which the $AuCl_4^-$

/BBPMA-H_2Cl^+ salt underwent reduction to form the $AuCl_2^-$/BBPMA-H_2Cl^+ salt (Figure 13).

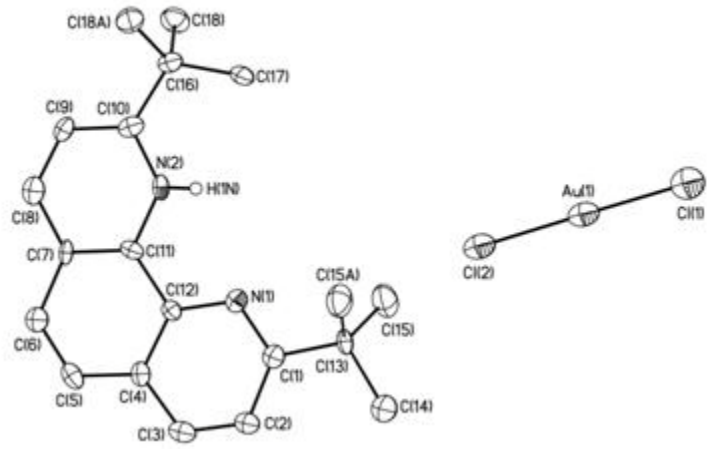

Figure 13. Molecular structure and numbering scheme of **5**. (35% probability) Hydrogen atoms have been omitted for clarity. Selected bond lengths (Å) and angles: Au-Cl···H–N 3.549, Au(1)–Cl(1) 2.258(4), Au(1)–Cl(2) 2.262(4), Cl(1)–Au(1)–Cl(2) 179.50(12).

Table 1. Crystal and refinement data for compounds **1-3**, **5**.

Complex	1	2	3	5
Empirical formula	C20 H25 Au Cl4 N2	C20 H25 Au Cl4 N2	C20 H24 Au Cl3 N2	C20 H25 Au Cl2 N2
Formula weight	632.19	632.19	595.73	561.29
Temperature K	160(2)	160(2)	173(2)	173(2)
Wavelength Å	0.71073	0.71073	0.71073	0.71073
Crystal system	Tetragonal	Triclinic	Triclinic	Orthorhombic
Space group	P4/n	P-1	P-1	Pnma
V/Å^3	4683.6(10)	1111.5(5)	3255.0(3)	2033.0(3)
Z	8	2	6	4
a/Å	24.553(3)	9.013(2)	14.3221(6)	27.523(2)
b/Å	24.553(3)	10.472(3)	15.3810(7)	6.7821(5)
c/Å	7.7689(12)	11.909(3)	15.9327(8)	10.8909(9)
α/ °	90	92.196(4)	107.374(4)	90
β/ °	90	93.497(4)	102.677(3)	90
γ/ °	90	97.375(4)	90.992(3)	90
D_{calc}/Mg m^{-3}	1.793	1.889	1.823	1.834
Reflections Collected	23975	8947	22063	22152
Independent Reflections	4157	3945	12705	2276
Max., Min., Transmission	0.5519 and 0.1733	0.4153 and 0.2243	0.7628 and 0.2151	0.8644 and 0.3153
Final R indices [I>2σ(I)]	R1 = 0.0443, wR2 = 0.1337	R1 = 0.0321, wR2 = 0.0772	R1 = 0.0605, wR2 = 0.1257	R1 = 0.0464, wR2 = 0.0883
R indices (all data)	R1 = 0.0771, wR2 = 0.1636	R1 = 0.0547, wR2 = 0.0871	R1 = 0.1094, wR2 = 0.1488	R1 = 0.1014, wR2 = 0.1071
Goodness of fit	1.091	1.036	1.013	1.008

3.3 Thioredoxin Reductase Inhibition and Cytotoxicity Assays

Cytotoxicity data was derived from existing Human Head and Neck(Tu212) and Human Lymph Node Squamous Cell Carcinoma (886LN) tumor cell lines. Previous studies have shown that, while highly cytotoxic, the unsubstituted phen $AuCl_2$ complex does not show particularly strong specificity against different tumor cell lines, essentially having a shotgun effect against numerous lines.[30] Therefore, of immediate note is that compound **4** not only exhibits very strong cytotoxic potential at micromolar concentrations, but also demonstrates variable potential against different cell lines while always remaining more potent than cisplatin (Figure 14).

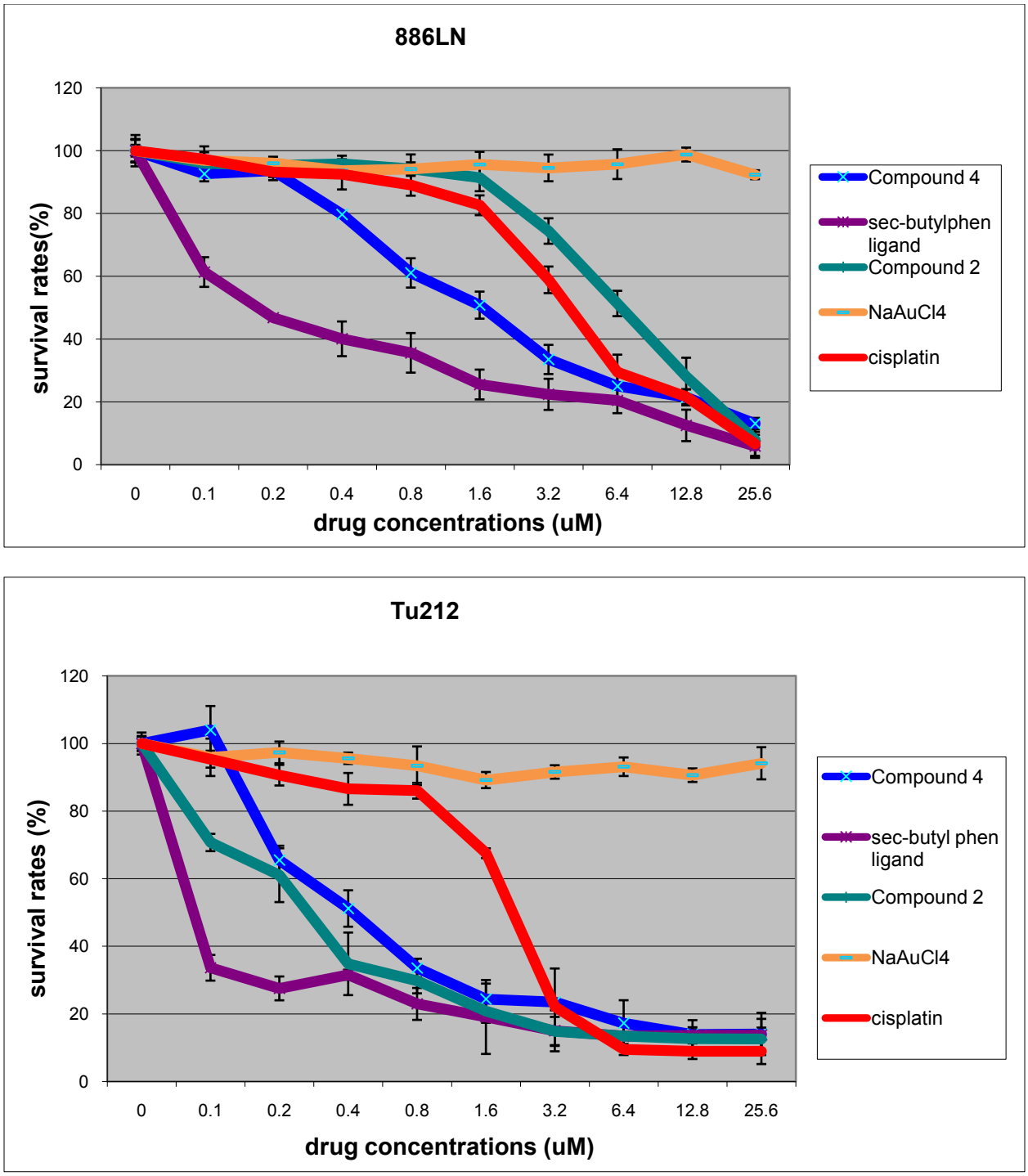

Figure 14. Cytotoxicity assays [sulforhodamine B (SRB) cytoxicity assay][5] on Tu212 (Human Head and Neck Tumors) and 886LN (Human Lymph Node Squamous Cell Carcinoma) for compounds **2** and **3** vs cisplatin, the *sec*-butyl phen ligand, and the $NaAuCl_4$ starting material.

In addition, the $NaAuCl_4$ starting material demonstrates essentially no cytotoxic potential in this concentration range. Cisplatin itself has an almost identical profile in both tumor cell lines, indicative of a similar mechanism of action in each line. However, compound **4**, in contrast to the phen $AuCl_2$, requires approximately five times the concentration to yield the same percent cell death in 886LN vs. Tu212. This is potentially a demonstration of variable potential in different tumor cell lines and a mechanism of action different from that of cisplatin or the planar phen $AuCl_2$. Of particular interest is that all compounds show lower IC50 values than cisplatin over a range of five different tumor cell lines, with the *sec*-butyl phen ligand showing dramatically lower values (Table 2).

Table 2. IC50 values for compounds 1 and 4, along with the sec-butyl phen ligand and cisplatin. H1703 and A549 = Human Lung Carcinomas, Tu212 and Tu686 = Human Head and Neck Tumors, and 886LN = Human Lymph Node Squamous Cell Carcinoma

	A549 (μM)	886LN (μM)	Tu212 (μM)	Tu686 (μM)	H1703 (μM)
1	0.37	1.13	0.16	0.38	0.09
4	0.76	1.6	0.34	1.16	0.2
Sec-butyl Phen Ligand	0.08	0.18	0.07	0.09	0.07
Cisplatin	3.1	4.2	2.7	2.9	7.9

Thioredoxin reductase inhibition assays indicate that all compounds synthesized are extremely effective at enzyme inhibition in an in vitro environment. Even nanomolar concentrations of compounds **1**-**4** dramatically reduce enzyme function (Figure 15), supporting the idea that gold(III) complexes derive their anticancer potential in the cellular environment by reducing mitochondrial function. Neither $AuCl_4^-$ ions nor the

free *sec*-butyl ligand appear to inhibit enzyme function at similar concentrations, highlighting the efficacy of the complexes against mitochondrial enzyme function.

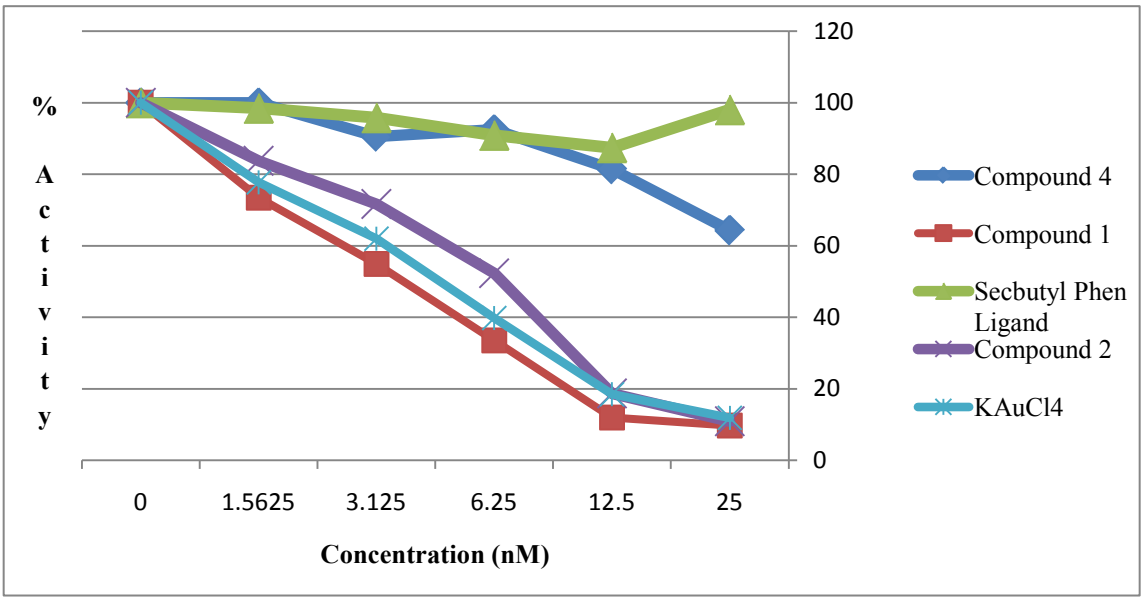

Figure 15. TrxR inhibition assay [50 nM recombinant rat TrxR1; enzyme activity monitored by 5,5'-dithio-bis(2-nitrobenzoic acid) (DTNB) reduction to TNB^- as determined by absorption at 412 nm).

3.4 Stability Data

As the gold(III) complexes will be tested for their anticancer properties, preliminary experiments to determine their stability in physiological buffer were carried out. In parallel experiments, compounds **2** and **4** were dissolved in a 3:1 isopropanol/acetonitrile solvent mixture, and then an aliquot of this solution for each compound was dissolved in phosphate buffer (0.1 M, pH 7.2) to make a final gold concentration of 1.0×10^{-5} M. These solutions were immediately analyzed by UV-Visible spectroscopy, and spectra were then collected hourly over a 24 hour period. With compounds **2** and **4**, there was a gradual decrease in the absorption maxima of the gold

complexes (Figure 16) After 24 hours, an observable, but immeasurable pale yellow precipitate was present in the cuvette.

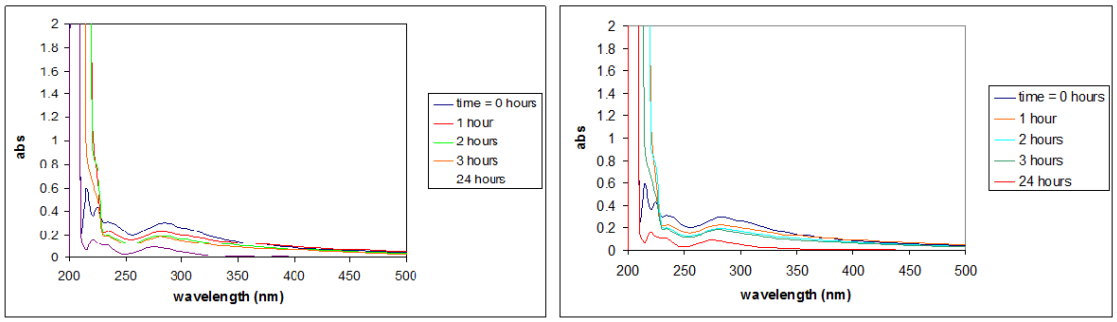

Figure 16. UV/vis spectra of compound **4** (left) and **2** (right) in phosphate buffer pH 7.2 over a 24 hour period (0.010 g of the solid gold complex was dissolved in 4.00 mL of a 3:1 2-propanal/acetonitrile solvent mixture temperature; an 8.0 uL aliquot of this solution was diluted in phosphate buffer to a final volume of 3.50 mL, which yielded a gold concentration of 1.0 x 10^{-5} M; spectra were collected at 20ºC).

Given that the hydrolysis of other gold(III) chloride species in aqueous buffer have been previously reported, this precipitate was assumed to be a gold(III) hydroxide species ($[Au(phen)(OH)_x(Cl)_y]$).[46] The formation of these hydrolysis products appear to be evidenced in the UV-Visible spectra, as the spectra taken after the initial scan indicate the presence of some intermediate complex, which after complete precipitation over a 24 hour period results in spectra which resemble those of the initial gold complexes, but at lower concentrations.

In an effort to corroborate this hypothesis, more concentrated samples of compound **4** (a dark orange solid) were prepared in both phosphate buffer and distilled water (5.0 x 10^{-4} M gold complex). A pale yellow precipitate formed in both water and phosphate buffer, though considerably less precipitate formed in the buffer solution. The pH of both solutions was measured immediately after the addition of the gold complex; the pH of the water solution dropped significantly (the pH after the addition of the gold

complex was 3.8), while the pH of the buffer solution did not change significantly. The decrease in pH in the gold complex/water solution seems to suggest the hypothesis that hydrolysis of the gold complex likely occurs in aqueous solution is true, as the formation of the hydroxo complex would generate H^+ ions (see Scheme 2). The solid precipitate from both solutions was then isolated and characterized by IR spectroscopy. The formation of the hydroxo complex was further confirmed by the presence of an intense OH stretch in the IR (3442 cm^{-1}). Also of note was the observation of =C-H stretches at 3069 cm^{-1}, and C=C stretches at 1594 cm^{-1} and 1624 cm^{-1}, indicative of the presence of the phen ligand on the gold hydroxo complex.

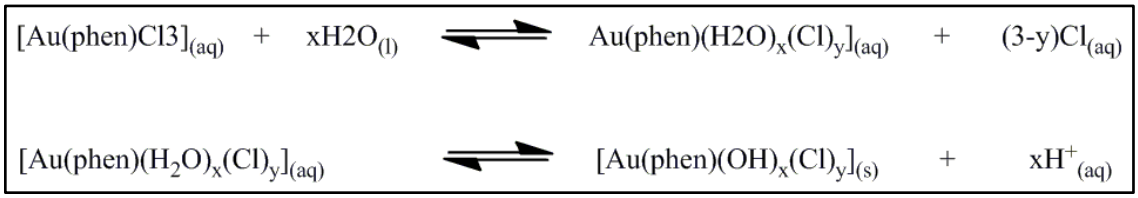

Scheme 2. Proposed mechanism of gold(III) hydroxo precipitate formation.

Even though gold(III)-chloride bonds are not completely inert in aqueous solution, the fact the gold-phen binding appears to be stable should provide an opportunity to extend the *in vitro* molecular design of this class of complexes to biological systems. Additionally, the fact the gold(III) hydroxo complexes demonstrated higher solubility in phosphate buffer fosters optimism that these gold compounds may show promise in future anticancer studies.

Our laboratory has also sought to apply the synthetic procedures applied here to other bipyridyl ligand-metal complexes. Conditions identical to those described here have recently been applied to produce a novel methyl-substituted bipyridine derivative

chelated to a gold center with a pseudo square-pyramidal structure similar to **3** and **4**, with the structure confirmed by X-ray crystallography studies (Figure 17). This result may indicate that the use of silver(I) salts as applied in this report to yield metal-chelation in bulky systems may also be applied to a range of analogous bis(N,N') donor ligands. Efforts are underway to extend this distinctive coordination geometry to gold(III) complexes with other ligand types, with Figure 17 demonstrating an early successful analogue.

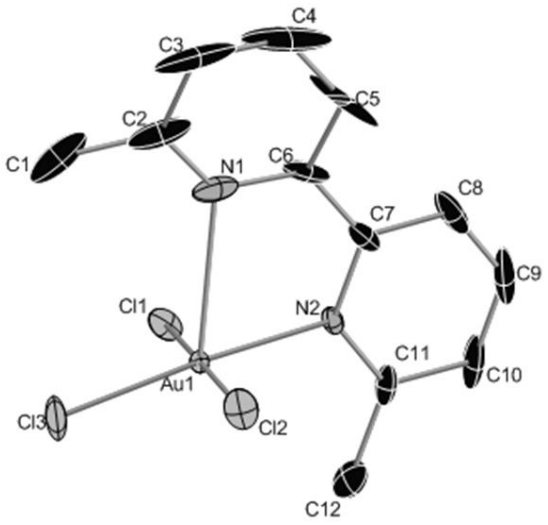

Figure 17. Molecular structure and numbering scheme of 6,6'-dimethyl-2,2'-bipyridine gold(III) trichloride coordination complex (35% probability). Hydrogen atoms have been omitted for clarity (unpublished structure).

4. Conclusions and Future Work

In summary, neutral square pyramidal gold(III) coordination compounds possessing substituted phen ligands have been synthesized and fully characterized. These compounds (**3** and **4**) represent rare examples of gold(III) complexes that bear bulky substituents on the 2,9- positions of phenanthroline, and have been obtained through a

modified synthetic route that uses silver(I) salts to help facilitate direct coordination of the ^{R}phen ligands. We have demonstrated that the choice of the synthetic conditions can have a dramatic impact on the type of gold(III) complex that can be obtained, and in particular have shown that the use of $HAuCl_4$ can lead to the formation of salts comprised of $[AuCl_4]^-$ anions and protonated $[^{R}PhenH]^+$ ligands (compounds **1** and **2**). The results of this research seem to indicate that the synthesis of gold(III) complexes that undergo direct coordination with 2,9-dialkylphen is limited to ligands that have methyl, 1°, or 2º carbons on the α-carbon of the alkyl substituent.

The successful synthesis of **3** and **4** may provide access to a class of gold compounds that can potentially be used as novel anticancer agents. Compound **3** has been shown to demonstrate cytotoxic potential across different tumor cell lines at concentration ranges similar to that of the highly efficacious cisplatin. In addition, it appears that this potential differs somewhat across each line, indicating potential specificity against different types of tumors. This report also demonstrates that such complexes are highly effective inhibitors of the selenocysteine containing enzyme thioredoxin reductase. Such early studies support the hypothesis that gold(III) complexes may find their mechanism of action through inhibition of mitochondrial function. The *sec*-butyl phen ligand itself demonstrates a strong cytotoxic potential, inhibiting cellular growth even at sub-micromolar concentrations.

Preliminary studies also show that the coordination complexes appear to be relatively stable at biological conditions for several hours. Further studies in these areas are ongoing in our laboratory, along with the synthesis of new types of gold(III) complexes in order to further explore the effect of structure on the specificity gold(III)

complexes containing bis(N,N') donor ligands. Specifically, new 6,6'-dialkyl-2,2'-bipyridine ligands are being synthesized due to preliminary data suggesting that such ligands produce gold complexes that are both more stable and more soluble in aqueous solution than their phen counterparts, and 5,6-dialkyl-1,10-phen ligands due to their potential to probe the phen aromatic region's interaction with DNA and the influence of structural changes at these positions on cytotoxicity (Figure 18).

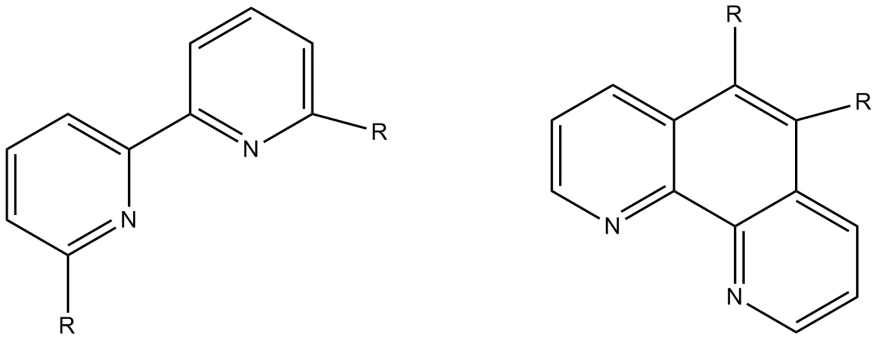

6,6'-dialkyl-2,2'-bipyridine 5,6-dialkyl-1,10-phenanthroline

Figure 18. Potential new bis(N,N') ligand designs.

5. References

(1) van Zutphen, S.; Reedijk, J. *Coordination Chemistry Reviews* **2005**, *249*, 2845.
(2) Sundquist, W. I.; Lippard, S. J. *Coordination Chemistry Reviews* **1990**, *100*, 293.
(3) Agarwal, A.; Balla, J.; Alam, J.; Croatt, A. J.; Nath, K. A. *Kidney Int.* **1995**, *48*, 1298.
(4) Hamers, F. P. T.; Brakkee, J. H.; Cavalletti, E.; Tedeschi, M.; Marmonti, L.; Pezzoni, G.; Neijt, J. P.; Gispen, W. H. *Cancer Research* **1993**, *53*, 544.
(5) Deegan, C.; Coyle, B.; McCann, M.; Devereux, M.; Egan, D. A. *Chemico-Biological Interactions* **2006**, *164*, 115.
(6) Kelland, L. R. *Cisplatin* **1999**, 497.
(7) Wang, G.; Reed, E.; Li, Q. Q. *Oncol Rep* **2004**, *12*, 955.
(8) Camm, K. D.; El-Sokkary, A.; Gott, A. L.; Stockley, P. G.; Belyaeva, T.; McGowan, P. C.; Gianferrara, T.; Bratsos, I.; Iengo, E.; Milani, B.; Ostric, A.; Spagnul, C.; Zangrando, E.; Alessio, E.; Gossens, C.; Tavernelli, I.; Rothlisberger, U.; Ruiz, J.; Vicente, C.; de Haro, C.; Bautista, D. *Dalton Trans* **2009**, *28*, 10914.
(9) Gianferrara, T.; Bratsos, I.; Iengo, E.; Milani, B.; Ostric, A.; Spagnul, C.; Zangrando, E.; Alessio, E. *Dalton Trans* **2009**, *28*, 10742.
(10) Gossens, C.; Tavernelli, I.; Rothlisberger, U. *J Phys Chem A* **2009**, *113*, 11888.

(11) Ivanov, M. A.; Puzyk, M. V.; Balashev, K. P. *Russ. J. Gen. Chem.* **2003**, *73*, 1821.
(12) Ruiz, J.; Vicente, C.; de Haro, C.; Bautista, D. *Dalton Trans* **2009**, *14*, 5071.
(13) Hartinger, C. G.; Zorbas-Seifried, S.; Jakupec, M. A.; Kynast, B.; Zorbas, H.; Keppler, B. K. *Journal of Inorganic Biochemistry* **2006**, *100*, 891.
(14) Gao, E.; Liu, C.; Zhu, M.; Lin, H.; Wu, Q.; Liu, L. *Anticancer Agents Med Chem* **2009**, *9*, 356.
(15) Zhao, G.; Lin, H. *Curr Med Chem Anticancer Agents* **2005**, *5*, 137.
(16) Fries, J. F.; Bloch, D.; Spitz, P.; Mitchell, D. M. *Am J Med* **1985**, *78*, 56.
(17) Messori, L.; Orioli, P.; Tempi, C.; Marcon, G. *Biochem. Biophys. Res. Commun.* **2001**, *281*, 352.
(18) Tiekink, E. R. T. *Critical Reviews in Oncology/Hematology* **2002**, *42*, 225.
(19) Ronconi, L.; Marzano, C.; Zanello, P.; Corsini, M.; Miolo, G.; Macca, C.; Trevisan, A.; Fregona, D. *Journal of medicinal chemistry* **2006**, *49*, 1648.
(20) Gabbiani, C.; Casini, A.; Messori, L. *Gold Bulletin (London, United Kingdom)* **2007**, *40*, 73.
(21) Carotti, S.; Marcon, G.; Marussich, M.; Mazzei, T.; Messori, L.; Mini, E.; Orioli, P. *Chemico-Biological Interactions* **2000**, *125*, 29.
(22) Milacic, V.; Chen, D.; Ronconi, L.; Landis-Piwowar, K. R.; Fregona, D.; Dou, Q. P. *Cancer Research* **2006**, *66*, 10478.
(23) Rigobello, M. P.; Messori, L.; Marcon, G.; Agostina Cinellu, M.; Bragadin, M.; Folda, A.; Scutari, G.; Bindoli, A. *J. Inorg. Biochem.* **2004**, *98*, 1634.
(24) Barnard, P. J.; Berners-Price, S. J. *Coordination Chemistry Reviews* **2007**, *251*, 1889.
(25) Wang, Y.; He, Q.-Y.; Che, C.-M.; Tsao, S. W.; Sun, R. W.-Y.; Chiu, J.-F. *Biochemical* **2008**, *75*, 1282.
(26) Karki, S. S.; Thota, S.; Darj, S. Y.; Balzarini, J.; De Clercq, E. *Bioorg Med Chem* **2007**, *15*, 6632.
(27) Thota, S.; Karki, S. S.; Jayaveera, K. N.; Balzarini, J.; Clercq, E. D. *J Enzyme Inhib Med Chem* **2010**, *3*, 3.
(28) Aguirre, J. D.; Angeles-Boza, A. M.; Chouai, A.; Turro, C.; Pellois, J. P.; Dunbar, K. R. *Dalton Trans* **2009**, *28*, 10806.
(29) Abbate, F.; Orioli, P.; Bruni, B.; Marcon, G.; Messori, L. *Inorg. Chim. Acta* **2000**, *311*, 1.
(30) Casini, A.; Kelter, G.; Gabbiani, C.; Cinellu Maria, A.; Minghetti, G.; Fregona, D.; Fiebig, H.-H.; Messori, L. *Journal of biological inorganic chemistry : JBIC : a publication of the Society of Biological Inorganic Chemistry* **2009**, *14*, 1139.
(31) Robinson, W. T.; Sinn, E. *J. Chem. Soc., Dalton Trans.* **1975**, 726.
(32) Pallenberg, A. J.; Koenig, K. S.; Barnhart, D. M. *Inorg. Chem.* **1995**, *34*, 2833.
(33) Hudson, Z. D.; Sanghvi, C. D.; Rhine, M. A.; Ng, J. J.; Bunge, S. D.; Hardcastle, K. I.; Saadein, M. R.; MacBeth, C. E.; Eichler, J. F. *Dalton Trans.* **2009**, 7473.
(34) Beltran, L. M. C.; Long, J. R. *Acc. Chem. Res.* **2005**, *38*, 325.
(35) Sheldrick, G. M. *Acta Crystallographica Section A* **2008**, *64*, 112.
(36) Skehan, P.; Storeng, R.; Scudiero, D.; Monks, A.; McMahon, J.; Vistica, D.; Warren, J. T.; Bokesch, H.; Kenney, S.; Boyd, M. R. *J Natl Cancer Inst* **1990**, *82*, 1107.
(37) Zhang, X.; Zhang, H.; Tighiouart, M.; Lee, J. E.; Shin, H. J.; Khuri, F. R.; Yang, C. S.; Chen, Z.; Shin, D. M. *International Journal of Cancer* **2008**, *123*, 1005.

(38) Wallenborg, K.; Vlachos, P.; Eriksson, S.; Huijbregts, L.; Arnér, E. S. J.; Joseph, B.; Hermanson, O. *Experimental Cell Research* **2009**, *315*, 1360.
(39) Cao, L.; Jennings, M. C.; Puddephatt, R. J. *Inorg. Chem.* **2007**, *46*, 1361.
(40) Ivanov, M. A.; Puzyk, M. V.; Tkacheva, T. A.; Balashev, K. P. *Russ. J. Gen. Chem.* **2006**, *76*, 165.
(41) Ade, A.; Cerrada, E.; Contel, M.; Laguna, M.; Merino, P.; Tejero, T. *J. Organomet. Chem.* **2004**, *689*, 1788.
(42) Aullon, G.; Bellamy, D.; Orpen, A. G.; Brammer, L.; Bruton, E. A. *Chem. Commun. (Cambridge)* **1998**, 653.
(43) Charlton, R. J.; Harris, C. M.; Patil, H.; Stephenson, N. C. *Inorg. Nucl. Chem. Lett.* **1966**, *2*, 409.
(44) O'Connor, C. J.; Sinn, E. *Inorg. Chem.* **1978**, *17*, 2067.
(45) Micklitz, W.; Lippert, B.; Mueller, G.; Mikulcik, P.; Riede, J. *Inorg. Chim. Acta* **1989**, *165*, 57.
(46) Calamai, P.; Carotti, S.; Guerri, A.; Messori, L.; Mini, E.; Orioli, P.; Speroni, G. P. *J. Inorg. Biochem.* **1997**, *66*, 103.